Biosensors and Bioelectronics ■ (■■■■) ■■■–■■■

Contents lists available at ScienceDirect

Biosensors and Bioelectronics

journal homepage: www.elsevier.com/locate/bios

Dopamine biosensor based on surface functionalized nanostructured nickel oxide platform

Appan Roychoudhury [a], Suddhasatwa Basu [b], Sandeep Kumar Jha [a,*]

[a] Centre for Biomedical Engineering, Indian Institute of Technology Delhi, Hauz Khas, New Delhi 110016, India
[b] Department of Chemical Engineering, Indian Institute of Technology Delhi, Hauz Khas, New Delhi 110016, India

ARTICLE INFO

Article history:
Received 29 August 2015
Received in revised form
19 November 2015
Accepted 20 November 2015

Keywords:
Dopamine biosensor
Neurochemical detection
NiO nanoparticles
Tyrosinase
Electrochemical sensor

ABSTRACT

A dopamine biosensor has been developed using nickel oxide nanoparticles (NPs) and tyrosinase enzyme conjugate. Nickel oxide (NiO) NPs were synthesized by sol–gel method using anionic surfactant, sodium dodecyl sulphate (SDS), as template to control the size of synthesized nanoparticles. The structural and morphological studies of the prepared NPs were carried out using X-ray diffraction (XRD), transmission electron microscopy (TEM) and dynamic light scattering (DLS) techniques. Afterwards, tyrosinase enzyme molecules were adsorbed on NiO NPs surface and enzyme coated NPs were deposited on indium tin oxide (ITO) coated flexible polyethylene terephthalate (PET) substrate by solution casting method. The formation of enzyme–NPs conjugate was investigated by atomic force microscopy (AFM) and Fourier transform infrared spectroscopy (FTIR) techniques and used in selective detection and estimation of neurochemical dopamine by electrochemical method. The fabricated Tyrosinase/NiO/ITO electrode exhibits high sensitivity of 60.2 nA/μM in linear detection range (2–100 μM) with a detection limit of 1.038 μM. The proposed sensor had a response time of 45 s, long shelf life (45 days) with good reproducibility and selectivity in presence of interfering substances and was validated with real samples. The tyrosinase enzyme functionalized NiO platform has good bio-sensing efficacy and can be used in detection of other catecholamines and phenolic neurochemicals.

1. Introduction

Dopamine is known to be a significant catecholamine neurotransmitter that shows important role in the functions of central and peripheral nervous system, renal and hormonal systems of human and other mammals (Heien et al., 2005; Wightman et al., 1988). It is produced by decarboxylation of 3,4-dihydroxy phenylalanine and operated as a precursor in the synthesis of neurotransmitters epinephrine and norepinephrine. Dopamine also acts as a neuromodulator in brain circuitry and responsible for several physiological conditions such as mood, behavior, memory, attention and movement (Robinson et al., 2003). Abnormal metabolism and concentration of dopamine in body can lead to neurological diseases like Parkinson's disease, schizophrenia, epilepsy, senile dementia and attention deficit hyperactivity disorder (ADHD) (Cao et al., 2008; Huffman and Venton, 2009; Mo and Ogorevc, 2001; Robinson et al., 2003; Wightman et al., 1988). Moreover in emergency condition, dopamine is infused to the patients showing the symptoms of myocardial infraction, hypertension, bronchial asthma and during acute heart surgery (Beitollahi et al., 2008). Due to such physiological and pathophysiological effects, it is essential to develop a quantitative method to accurately estimate dopamine for diagnosis and continuous monitoring of neurological disorders.

The currently available analytical methods for dopamine determination are high performance liquid chromatography (Carrera et al., 2007; Muzzi et al., 2008), UV spectrometry (Barreto et al., 2008), capillary electrophoresis (Kang et al., 2005; Li et al., 2010; Thabano et al., 2009), liquid chromatography-electrospray tandem mass spectrometry (El-Beqqali et al., 2007), flow injection analysis with spectrophotometric detection (Deftereos et al., 1993), coulometric (Myers et al., 1998), fluorescence (Chen et al., 2011; Khattar and Mathur, 2013; Nikolelis et al., 2004) and electrochemical detection (Chen and Peng, 2003; Matos et al., 2000; Mecker and Martin, 2008; Umasankar and Chen, 2008; Zhang et al., 2013). Apart from electrochemical detection, most of the procedures are complex, cumbersome, expensive, time consuming and requires lots of sample. Due to electrochemical activity, dopamine can be efficiently detected by applying appropriate potential across the electrodes (Njagi et al., 2010). With this in view, enzyme biosensor combined with electrochemical detection may be advantageous owing to rapid detection, simplicity and ease in miniaturization.

* Corresponding author.
E-mail address: sandeepjha@cbme.iitd.ac.in (S.K. Jha).

http://dx.doi.org/10.1016/j.bios.2015.11.061
0956-5663/

Further, for reliable and rapid determination of dopamine and to increase sensitivity and selectivity of the biomedical devices, enzyme can be proficiently used as biorecognition element. Tyrosinase or polyphenol oxidase (EC 1.14.18.1) is binuclear copper containing enzyme that catalyzes oxidation of phenolic compounds in two steps to their respective *o*-quinones, which is further reduced at appropriate redox potential to form original phenols again (Tembe et al., 2008; Zhou et al., 2007). *o*-quinones are electroactive species and can be reduced at moderately negative potential (Tembe et al., 2006; Zhou et al., 2007) which is helpful in the prevention of the polymerization of phenols and interferences from oxidizable species (Koile and Johnson, 1979). Dopamine is a catechol like phenolic substance, can be detected with enhanced specificity using tyrosinase enzyme molecules through direct reduction of bio-catalytically liberated *o*-dopaquinone species (Njagi et al., 2010; Tsai and Chiu, 2007; Zhou et al., 2007).

For suitable immobilization of tyrosinase enzyme molecules, several materials such as graphite (Nistor et al., 1999), conducting polymer (Arslan et al., 2005; Rajesh et al., 2004), nafion membrane (Furbee Jr et al., 1993), carbon paste (Caruso et al., 1999), hydrogel (Daigle and Leech, 1997) and biopolymers (Liu et al., 2005) have been used as matrices to improve stability of the enzyme in sensor probe. Most of these matrices used to develop tyrosinase based system suffer from complexity and reduced sensitivity (Tembe et al., 2008, 2006). In this context, nanostructured metal oxides can be effectively used as matrices for biomolecule immobilization due to presence of fascinating electrochemical and optical properties, catalytic effects and efficient charge transfer abilities from biomolecules to a particular substrate (Doong and Shih, 2010; Thanh and Green, 2010). Nanostructured metal oxides have attracted plentiful attention of the researchers owing to their adsorption capabilities, effective surface area for biomolecule immobilization with desired orientation and better conformation that leads to high biological activity of the immobilized bio-sensing molecules (Caruso, 2001; Solanki et al., 2011). Among the various nanostructured metal oxides, nickel oxide nanoparticles have recently been used in bio-sensing application (Li et al., 2008) due to the presence of high electro-catalytic activity, fast electron transport property, high surface energy, chemical stability, low cost and biocompatibility (Ali et al., 2013; Kavitha and Yuvaraj, 2011; Salimi et al., 2007). In addition the existence of variable oxidation states in nickel oxide nanoparticles helps in easy mobility of the electrons (Mohan et al., 2011). Beside this, high isoelectric point (IEP 10.8) of NiO nanoparticles make it suitable for tyrosinase enzyme (IEP 4.7) immobilization. The NiO nanoparticles can be synthesized through sol–gel, reverse micelle, microwave irradiation and laser induced fragmentation method (Justin et al., 2010; Singh et al., 2011). In sol–gel method NiO nanoparticles are generally prepared by using non-ionic, anionic and cationic surfactants to control pore volume, surface area, crystallite size and organization of NiO nanocrystals (Justin et al., 2010). Among three types of surfactants, the anionic surfactant shows finest result in respect of higher surface redox activity, lower crystallite size, porous morphology and higher surface area (Justin et al., 2010). These properties are possibly most suitable for biomolecule immobilization and electrochemical measurement. Hence in our experiment sodium dodecyl sulphate (SDS) has been used as anionic surfactant during synthesis of NiO nanoparticles.

The electrochemical detection of dopamine is greatly affected by the presence of co-existing interfering substances ascorbic acid and uric acid because of similarity in oxidation potential of dopamine close to these interfering species (Liu et al., 2013; Zhang et al., 2005). Dopamine requires higher oxidation potential (between 0.5 and 0.7 V) which includes oxidation range of many other electrochemically active species (Njagi et al., 2010). To avoid the effect of interferents, tyrosinase based system has been used in selective and specific detection of dopamine and the estimation of dopamine has been monitored through direct reduction of *o*-dopaquinone species at relatively lower potential (~ -0.15 V).

In the present study, sol–gel method with anionic surfactant SDS has been used to synthesize NiO nanoparticles (NPs) and tyrosinase enzyme has been immobilized on synthesized NiO NPs by physio-adsorption technique. The NiO NPs-tyrosinase conjugates, characterized by different methods, was then deposited on indium tin oxide (ITO) coated polyethylene terephthalate (PET) substrate by solution casting method. These enzyme strips were used for biosensor measurements and several optimization steps were performed to characterize the dopamine biosensor in synthetic samples, with interferents and in real sample.

2. Experimental section

2.1. Materials and reagents

Tyrosinase (EC 1.14.18.1 from *Agaricus bisporus* with activity of 1000 U/mg of solid), dopamine hydrochloride ($C_8H_{11}NO_2 \cdot HCl$), Poly (vinyl alcohol) (PVA, MW 130000), ITO coated PET substrate and sodium hydroxide pellets (NaOH) were procured from Sigma–Aldrich (USA). Nickel nitrate hexahydrate [$Ni(NO_3)_2 \cdot 6H_2O$] and sodium dodecyl sulphate ($NaC_{12}H_{25}SO_4$) were purchased from Alfa Aesar (UK). The stock solution of tyrosinase (1 mg/mL) was freshly prepared in phosphate buffer (50 mM, pH 6.5). All solutions used in this study were prepared with deionized water of resistivity not less than 18 MΩcm, obtained from Milli-Q water purification system (Milli-Q, USA).

2.2. Synthesis of nickel oxide (NiO) nanoparticles (NPs)

Nickel oxide nanoparticles (NiO NPs) were synthesized by co-precipitation method using sodium dodecyl sulphate (SDS) as anionic surfactant. For this purpose, 20 mM of $[Ni(NO_3)_2] \cdot 6H_2O$ and 40 mM of NaOH were dissolved in deionized water (DW) individually and magnetically stirred for one hour to obtain homogenous and transparent solutions. 10 mM of SDS was added in 20 mM of $[Ni(NO_3)_2] \cdot 6H_2O$ solution and stirred for another one hour. The aqueous solution of NaOH was added drop wise into the resultant solution up to pH ~11.5–12 and kept under constant stirring for 2 h at room temperature (25 °C). A light green precipitate of $Ni(OH)_2$ thus obtained was separated by centrifugation and washed 3–4 times with DW and ethanol. The precipitate was then oven-dried at 70 °C for 24 h and calcined at 300 °C for 3 h to obtain NiO NPs. The reaction mechanism involved in the synthesis of NiO NPs is shown in (Eqs. (1) and 2)

$$Ni(NO_3)_2 + 2NaOH \rightarrow Ni(OH)_2 \downarrow + 2NaNO_3 \quad (1)$$

$$Ni(OH)_2 \xrightarrow[300\ ^\circ C \text{ for } 3 \text{ hrs}]{\Delta} NiO + H_2O \quad (2)$$

2.3. Nanoparticle characterization

The as-prepared NPs were characterized using various techniques to ascertain composition, homogeneity, particle sizes etc. The X-ray diffraction (XRD) spectra of the synthesized NiO NPs were obtained from X-ray diffractometer (Rigaku, MiniFlex 600) with CuKα radiation at $\lambda = 1.5406$ Å [range (20–80°) and scan rate 4°/min]. The structural and morphological properties of NiO NPs were investigated using transmission electron microscopy (TEM, FEI TECNAI G^2S TWIN), dynamic light scattering (DLS, Malvern Zetasizer NanoZS90 particle size analyzer) and energy dispersive X-ray

Please cite this article as: Roychoudhury, A., et al., Biosensors and Bioelectronics (2015), http://dx.doi.org/10.1016/j.bios.2015.11.061

spectroscopy (EDS, JEOL JSM-6010LA) studies. The surface morphological studies of NiO/ITO and Tyrosinase/NiO/ITO electrodes were performed using atomic force microscopy (AFM, Bruker dimension icon with Scan Assist). FT-IR spectra of the NPs and NPs-enzyme conjugate were recorded with FTIR spectrophotometer (Bruker Vertex 70v).

2.4. Immobilization and preparation of electrodes

For the preparation of Tyrosinase/NiO/ITO bioelectrodes, first Tyrosinase-NiO NPs conjugate was prepared by uniformly dispersing NiO NPs in tyrosinase enzyme solution (1 mg/mL phosphate buffer saline, pH 6.5) followed by incubation for 2 h. The enzyme conjugated NPs were separated through centrifugation and washed with phosphate buffer saline (PBS) to remove unbound enzyme molecules. The tyrosinase enzyme molecules got immobilized on the NiO NPs through physio-adsorption. The tyrosinase conjugated NiO NPs were then dispersed in PBS (pH 6.5) contained with 50% absolute ethanol for uniform, thin film formation on indium-tin-oxide (ITO) coated polyethylene terephthalate (PET) substrate. The optimized volume 20 μL of enzyme-NPs conjugate soln. was deposited uniformly onto 1 cm × 1 cm dimension of ITO surface by solution casting method and kept undisturbed in humid condition (4 °C) for 12 h. The Tyrosinase/NiO/ITO bioelectrodes were rinsed with ice cold PBS (50 mM, pH 6.5) to remove unbound particles and stored in 4 °C when not in use.

The NiO/ITO electrodes were prepared using same methodology without adding tyrosinase enzyme molecules. Finally, both Tyrosinase/NiO/ITO and NiO/ITO electrodes were dipped in 0.25% of polyvinyl alcohol (PVA) solution and dried overnight and used for further detection of dopamine. This additional step was performed to prepare a thin hydrophilic polymer coating layer in order to prevent desorption and loss of enzyme from electrode surface during dopamine detection in electrolyte solution. Moreover, coating of PVA solution was helpful to stabilize immobilized enzymes onto electrode surface and increased shelf life of the fabricated electrodes. The NiO/ITO electrodes were prepared using same methodology for better comparison of the electrode surface before and after immobilization of tyrosinase enzyme. The stepwise fabrication of the bio-sensing platform is shown in Scheme S1 **in Supplementary Information**.

2.5. Biosensor studies

The electrochemical characterization of the fabricated electrodes and amperometric measurements were conducted on electrochemical analyzer (Biologic Science Instruments SP-150) using three-electrodes system with Tyrosinase/NiO/ITO as working electrode, a platinum (Pt) wire as counter electrode and saturated Ag/AgCl electrode as a reference electrode in 50 mM PBS of pH 6.5. For this, first, CV of bare ITO, NiO/ITO and Tyrosinase/NiO/ITO electrodes were recorded for 10 cycles at 100 mV/s scan rate in the potential range of −1 to +1.5 V using PBS (50 mM, pH 6.5, 0.9% NaCl) as electrolyte. Then 100 μL of 0.1–500 μM dopamine solutions were added to electrochemical cell and CV was recorded with each sample using Tyrosinase/NiO/ITO electrode under same conditions in order to get the calibration curve. Real sample analysis was performed by spiking bovine serum with known dopamine concentrations and then calculating the dopamine level using calibration curve obtained with synthetic dopamine samples. For studies with interferents, an additional 100 μL of interferents was added into the solution while keeping dopamine concentration fixed.

3. Results and discussion

3.1. Nanoparticle characterization

The NiO NPs were characterized using various techniques to ascertain their composition, homogeneity and sizes.

3.1.1. X-ray diffraction (XRD) studies

The XRD pattern of NiO NPs (Fig. 1A) reveals cubic (fcc) NiO phase with lattice parameter $a=4.1$ Å(space group: $Fm3m$). All the diffraction peaks corresponding to (111), (200), (220) and (222) planes are assigned with JCPDS card no. 73-1523 (Smith, 1936) and confirm the formation of highly crystalline, cubic structure of NiO NPs. No reflections of any impurity related to $Ni(OH)_2$, NiOOH, NiO_2, Ni_2O_3 could be detected, suggesting purity and single crystalline nature of the sample. The result also indicates complete transformation of $Ni(OH)_2$ to NiO and H_2O at 300 °C. The average crystallite size for the most intense peak (200) is calculated as 10 nm using Debye–Scherrer formula [Eq. (3)].

$$d=0.89\lambda/\beta cos\theta \quad (3)$$

where, λ (1.54060 Å) is the wavelength of X-ray, β is full width at half maxima (FWHM) of the diffraction peak, θ is glancing angle.

3.1.2. Transmission electron microscopy (TEM) studies

The shape and size of synthesized NiO NPs were studied using transmission electron microscopy (TEM) studies. Uniform colloidal solution of the NiO NPs was prepared and deposited on a carbon coated copper grid prior to study. The results show (Fig. 1C and D) that the particles are randomly oriented and semi-spherical in shape with average particle size varies from 25–30 nm. The selected area electron diffraction (SAED) pattern of NPs reveals corresponding diffraction rings in different radii (Fig. 1B) and the diameter of diffraction rings is proportional to $\sqrt{(\boldsymbol{h}^2+\boldsymbol{k}^2+\boldsymbol{l}^2)}$. The first, second, third and fourth rings represent to the (111), (200), (220) and (311) planes respectively.

3.1.3. Dynamic light scattering (DLS) studies

The particle size of the prepared NiO NPs was also measured from particle size distribution plot (Fig. 2A) obtained from dynamic light scattering (DLS) study. The result shows that the mean particle size is 40 nm with polydispersity index (PDI) of 0.571. It can be observed that the result is in strong agreement with TEM result and suggests uniform size distribution of the synthesized NiO NPs.

3.1.4. Energy dispersive X-ray spectroscopy (EDS) studies

The Energy dispersive X-ray spectroscopy (EDS) study was conducted for elemental analysis of the synthesized NPs. The EDS spectrum (Fig. 2B) shows corresponding peaks of nickel and oxygen and confirms the presence of two elements in synthesized nanomaterials. No other peaks of the impurities could be detected, indicating purity of the sample. Table S1 **in Supplementary Information** illustrates the percentage of elements present in the prepared NPs.

3.1.5. Fourier transform infrared spectroscopy (FT-IR) studies

The FT-IR spectra of the sol–gel derived NiO NPs is shown in Fig. 2C. The FTIR spectra of NiO NPs reveal broad peak for metal oxide stretching vibration mode at 557 cm^{-1} and 714 cm^{-1}, which confirms that the synthesized product is NiO NPs. The peaks arise at 1090 cm^{-1} and 1238 cm^{-1} are due to adsorbed carbonate moieties (C–O stretching vibration) and adsorbed C–OH moieties respectively. After immobilization of enzymes in Tyrosinase-NiO NPs conjugate (Fig. 2D), the peak for metal oxide stretching

Please cite this article as: Roychoudhury, A., et al., Biosensors and Bioelectronics (2015), http://dx.doi.org/10.1016/j.bios.2015.11.061

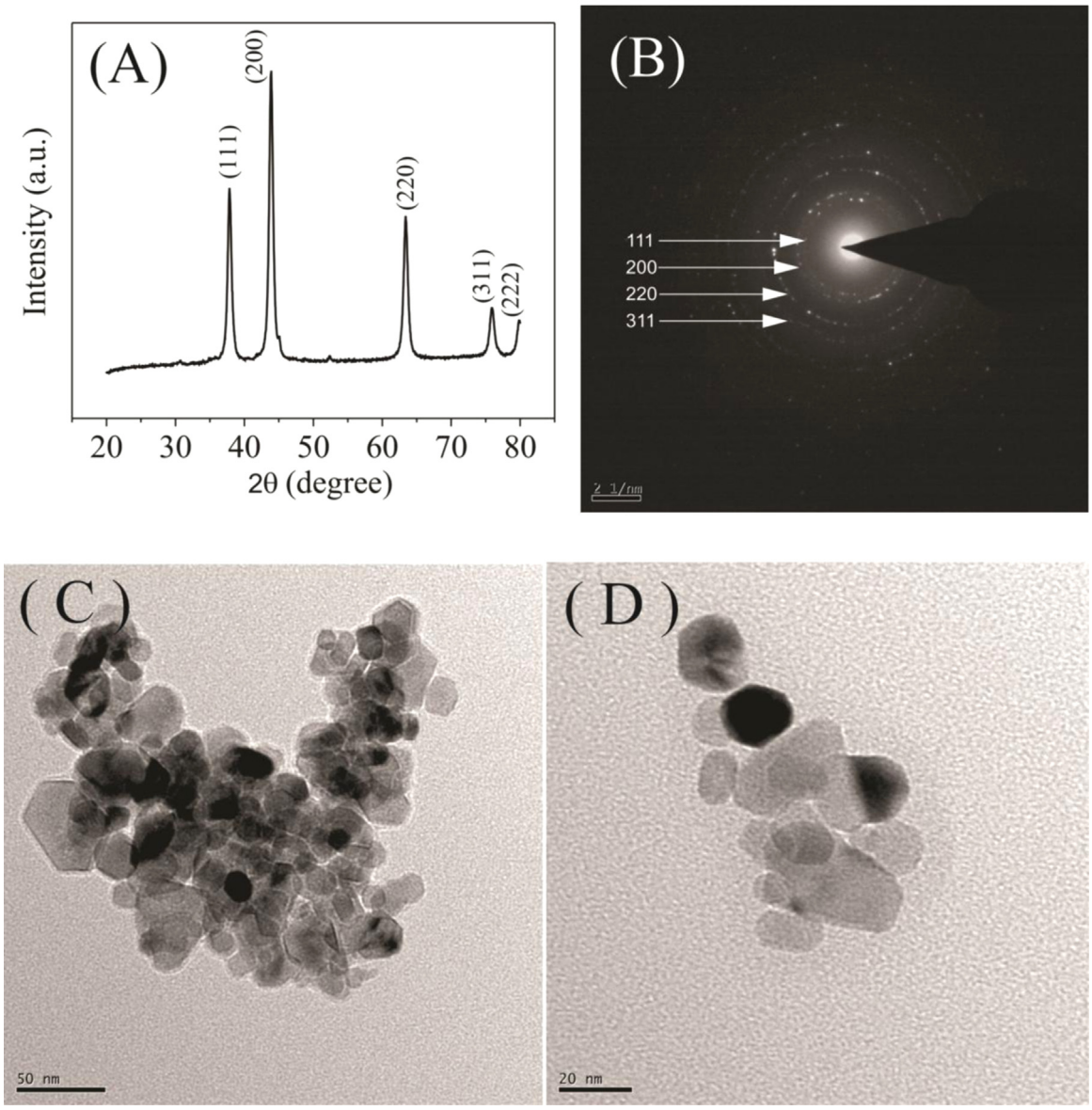

Fig. 1. Nanoparticle characterization: (A) X-ray diffraction and (B) SAED pattern of synthesized NiO NPs; (C and D) TEM micrographs of NiO NPs.

vibration mode shifts to 645 cm^{-1}. The peak at 1072 cm^{-1} is due to C–O stretching absorption, whereas the peak at 1405 cm^{-1} is for O–H stretching mode. The peaks observed at 1657 cm^{-1} and 1526 cm^{-1} originate from amide bonds in protein, suggesting the presence of enzyme due to C–O stretching of amide bond.

3.1.6. *Atomic force microscopy (AFM) studies*

Surface morphologies of the NiO/ITO and Tyrosinase/NiO/ITO electrodes were studied by atomic force microscopy (AFM) studies. The AFM micrograph of NiO/ITO electrode (Figure S1A **in Supplementary Information)** displays rough surface with uniformly oriented nanoporous granular morphology. After immobilization of tyrosinase enzyme molecules, the nanoporous granular morphology of NiO/ITO surface converts into regular smooth globular morphology (Figure S1B **in Supplementary Information)**. The NiO NPs film provides nanoporous surface, causing enhanced enzyme loading on NiO/ITO electrode and the immobilization of enzymes perhaps occurred due to electrostatic interaction between positively charged Ni^{2+} ions on the NiO/ITO surface and negatively charged carboxyl group (COO^-) of tyrosinase enzyme molecules. The R_q (root mean square roughness) value of Tyrosinase/NiO/ITO electrode increases to 70.3 nm as compared to R_q value of 12.6 nm for NiO/ITO electrode, indicating immobilization of the tyrosinase enzyme molecules on NiO surface. The enhancement of R_a (average peak height) for Tyrosinase/NiO/ITO electrode to 54.9 nm from 10.2 nm of previous NiO/ITO surface also confirms immobilization of the enzymes.

3.2. *Biosensor studies*

Upon immobilization, the value of Michaelis–Menten constant (K_m) for the enzyme at the fabricated Tyrosinase/NiO/ITO electrode has been estimated as 45.91 μM from Hanes-Wolf plot. The obtained low K_m value suggests high affinity of the Tyrosinase/NiO/ITO electrode towards the substrate and NiO NPs facilitate enzymatic reaction between tyrosinase and dopamine with higher enzyme activity. The fabricated electrodes were further used in biosensing of dopamine using cyclic voltammetric technique.

3.2.1. *Studies using cyclic voltammetry (CV)*

The cyclic voltammetry studies of bare ITO, NiO/ITO and Tyrosinase/NiO/ITO electrodes were conducted in PBS (50 mM, pH

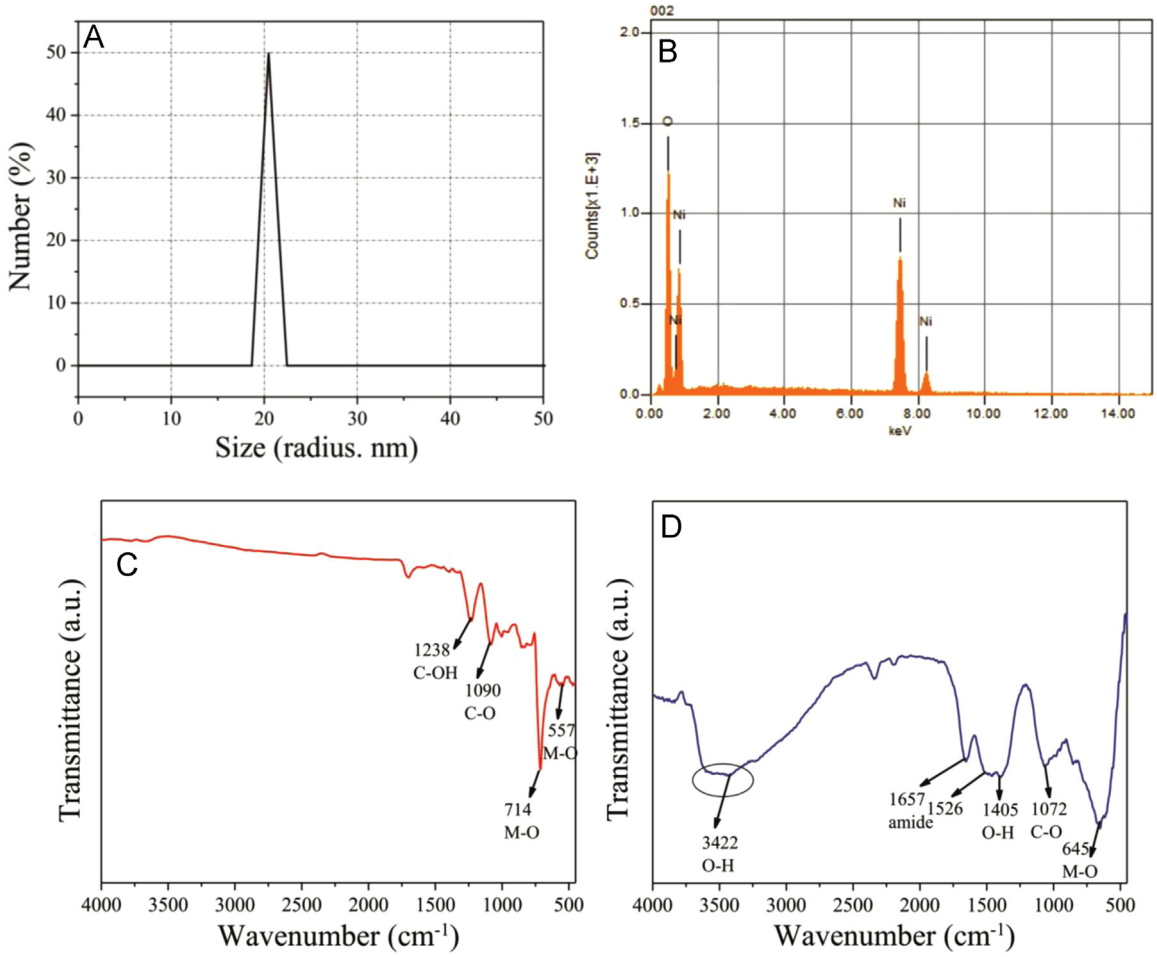

Fig. 2. Nanoparticle characterization: (A) Particle size distribution plot for NiO NPs acquired from DLS studies; (B) Energy dispersive X-ray spectra (EDS) of the NiO NPs; (C) FTIR spectra of NiO NPs; (D) FTIR spectra of Tyrosinase-NiO NPs conjugate.

6.5, 0.9% NaCl) at 100 mV/s scan rate in the potential range of −1.0 V to +1.5 V. The number of cycles for dopamine detection in cyclic voltammetry studies was optimized at constant scan rate and in presence of same dopamine concentration. It has been observed that after 10th cycles, peak current (I_{pa}) for dopamine oxidation and peak current (I_{pc}) for *o*-dopaquinone reduction became almost saturated (Figure S2 **in Supplementary Information**). However, we would like to clarify that it is a complete redox process and *o*-dopaquinone concentration reduces in each cycle and after 10th cycle it becomes stable. Thus, for all CV measurements, 10th cycle was chosen.

The results of CV studies (Fig. 3A) show no definite peaks for bare ITO, NiO/ITO and Tyrosinase/NiO/ITO electrodes (curve a to c) when the substrate dopamine (DA) was absent in the sample. This is attributed to non-occurrence of any redox reaction in the absence of substrate species in mediator free electrolyte. However, after inclusion of 100 μM dopamine solution, the redox peaks for dopamine oxidation and quinone reduction appeared for Tyrosinase/NiO/ITO electrode (curve d). Although a distinct peak appears to have emanated at −0.7 V, which did not appear in bare ITO, NiO/ITO and Tyrosinase/NiO/ITO electrodes, it clearly indicates that the peak at −0.7 V is only due to the presence of any intermediate product of dopamine redox process. Though, it is not clear which specie contributed towards it. Most of the present studies for reduction of *o*-dopaquinone during dopamine detection have focused on narrow potential range, not extending beyond −0.7 V. *o*-quinones are electroactive species and can be reduced at moderately negative potential (Tembe et al., 2006; Zhou et al., 2007) which is helpful in the prevention of the polymerization of phenols and interferences from oxidizable species (Koile and Johnson, 1979). The detection of dopamine can be executed with enhanced specificity using tyrosinase enzyme molecules through direct reduction of bio-catalytically liberated *o*-dopaquinone species (Njagi et al., 2010; Tsai and Chiu, 2007; Zhou et al., 2007). Moreover, the electrochemical detection of dopamine is greatly affected by the presence of co-existing interfering substances ascorbic acid and uric acid because of similarity in oxidation potential of dopamine close to these interfering species (Liu et al., 2013; Zhang et al., 2005). Dopamine requires higher oxidation potential (between 0.5 and 0.7 V) which includes oxidation range of many other electrochemically active species (Njagi et al., 2010). To avoid the effect of interferents, tyrosinase based system has been used in selective and specific detection of dopamine and the estimation of dopamine has been monitored through direct reduction of *o*-dopaquinone species at relatively lower potential (~ −0.15 V). Therefore we have only focused on cathodic (I_{pc}) peak currents for *o*-dopaquinone reduction at −0.16 V and the peak current enhances with increasing concentration of dopamine (Fig. 4A).

The reaction mechanism for electrochemical detection of dopamine is shown in Eq. (4)

$$\text{Dopamine} \underset{2e^-}{\overset{\text{Tyrosinase}}{\rightleftharpoons}} \text{Dopamine–}o\text{–quinone} + 2H^+ \quad (4)$$

Although, dopamine by itself an electroactive compound and can have redox peaks at most of the electrodes, just like other

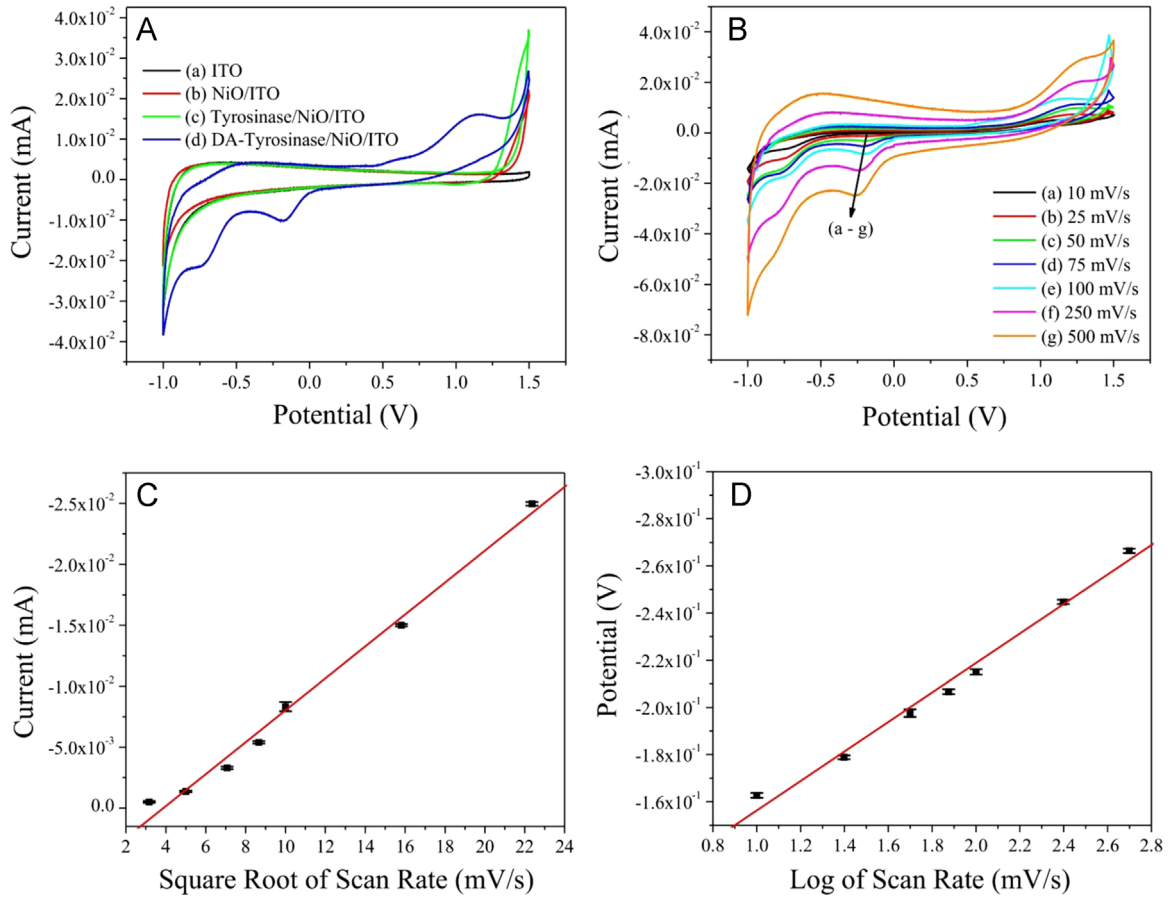

Fig. 3. (A) Cyclic voltammograms of (a) bare ITO; (b) NiO/ITO; (c) Tyrosinase/NiO/ITO; (d) Tyrosinase/NiO/ITO electrodes in presence of 100 μM dopamine; (B) Cyclic voltammogram of the Tyrosinase/NiO/ITO electrode with varying scan rate between 10 and 500 mV/s; (C) Calibration curve of the biosensor based on cathodic peak current of *o*-dopaquinone reduction as a function of square root of scan rate; (D) Calibration curve of biosensor based on *o*-dopaquinone reduction peak potential with logarithmic function of scan rate.

phenolic compounds (Njagi et al., 2010); the presence of tyrosinase in the reaction, as a biocatalyst enhances the kinetics of reaction and hence leads to higher sensitivity of detection. In our studies with ITO and NiO/ITO electrodes **(**Figure S3 **in Supplementary Information,** curve a and b respectively**)** redox peaks in the presence of dopamine appeared as expected, due to catalytic activity of metal oxide with respect to phenolic group. However, the outcome of CV studies in presence of dopamine **(**Figure S3 **in Supplementary Information)** indicates that the magnitude of peak current during reduction of *o*-dopaquinone (*Ipc,* 10.27 μA) of Tyrosinase/NiO/ITO electrode (curve c) is ~38% higher than the peak current (*Ipc,* 7.46 μA) with NiO/ITO electrode (curve b). This is due to availability of active-binding sites in enzyme and enhanced electron transfer between active sites of the enzyme and electrode that helps in sensitive detection of dopamine. The significant enhancement of peak current indirectly adds to the selectivity and specificity of detection, as interfering compounds would show much lower redox currents compared to that from ongoing reaction between tyrosinase and dopamine. Besides, the NiO NPs provide higher electrocatalytic activity, increased surface area and surface energy that facilitate better electron conduction between immobilized enzymes and transducer.

The detailed CV studies of Tyrosinase/NiO/ITO electrode were carried out as a function of scan rate varying from 10–500 mV/s in presence of 100 μM dopamine solution (Fig. 3B). The magnitude of cathodic (I_{pc}) peak currents for *o*-dopaquinone reduction increase linearly with square root of scan rate ($\upsilon^{1/2}$), suggesting improved electrocatalytic behavior (Fig. 3C). The shift of *o*-dopaquinone reduction peaks towards negative applied potential with increasing scan rate indicates a uniform facile charge transfer. This is attributed to the presence of NiO NPs on ITO surface that promotes electron transfer between enzyme and substrate. The values of the slope, intercept and regression co-efficient are given in Eq. (5)

$$I_{pc}[\mu A] = 5.08[\mu A] - 1.31[(\mu A)^2.\ s/mV]^{1/2} \times [\text{scan rate } (mV/s)]^{1/2} \quad \text{with } R^2 = 0.99 \tag{5}$$

The surface concentration of ionic species on NiO/ITO and Tyrosinase/NiO/ITO electrodes have been calculated from Brown–Anson model (Eq. (6)) (Singh et al., 2013).

$$I_p = n^2F^2\gamma Av/4RT \tag{6}$$

where I_p is peak current, n is the number of electrons transferred (1), F is Faraday constant (96485 C/mol), γ is the surface concentration of ionic species of the corresponding electrode (mol/cm^2), A is the surface area of the electrode (1 cm^2), v is the scan rate (100 mV/s), R is gas constant (8.314 J /mol k) and T is the room temperature (25 °C). It has been found that surface concentration of ionic species on Tyrosinase/NiO/ITO electrode (1.09×10^{-10} mol/cm^2) is higher than that of the NiO/ITO electrode (0.79×10^{-10} mol/cm^2). The diffusion co-efficient value (D) of electrolyte solution to the corresponding electrode surface has been determined using Randles–Sevcik equation (Eq. (7)) (Singh et al., 2013).

$$I_p = (2.69 \times 10^5)n^{3/2}AD^{1/2}Cv^{1/2} \tag{7}$$

where, D is diffusion co-efficient and C is surface concentration in

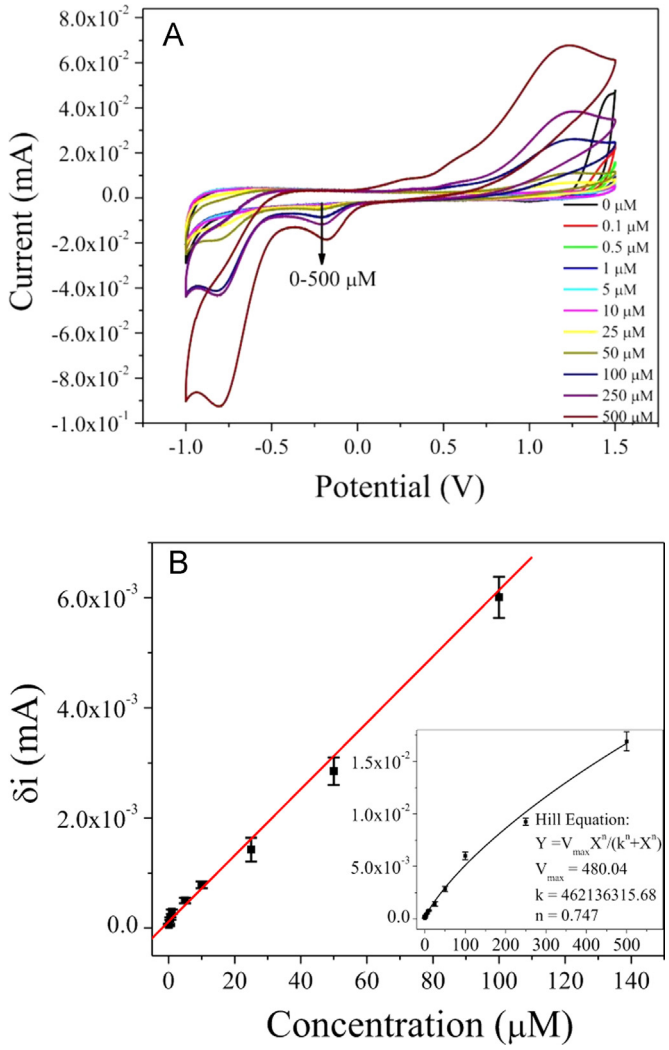

Fig. 4. (A) Electrochemical response of Tyrosinase/NiO/ITO electrode at different concentration of dopamine (0–500 μM); (B) Calibration curve of biosensor using cathodic peak currents for *o*-dopaquinone reduction: linear concentration (2–100 μM) range, (inset) whole concentration range (0.1–500 μM).

mol (50 mM). The diffusion co-efficient value for Tyrosinase/NiO/ITO electrode (5.79×10^{-12} cm^2/s) is higher as compared to NiO/ITO electrode (3.08×10^{-12} cm^2/s) (Table S2 **in Supplementary Information**). The electroactive surface area (A_e) of Tyrosinase/NiO/ITO electrode has been obtained using Randles–Sevcik equation and calculated diffusion co-efficient value.

$$A_e = S/(2.99 \times 10^5)n^{3/2}CD^{1/2} \quad (8)$$

where, S is the slope of straight line obtained from Eq. (5). The A_e value for Tyrosinase/NiO/ITO electrode has been estimated as 0.36 mm^2.

It can be seen from Fig. 3D, that the peak potential shows linear dependence with logarithmic function of scan rate. The value of electron transfer co-efficient (α) and n (number of electrons involved in the redox reaction) can be calculated from slope of the straight line equal to $-2.3RT/\alpha nF$ for the cathodic peak (Laviron, 1979) using Laviron's equation. For Tyrosinase/NiO/ITO electrode, electron transfer co-efficient (α) has been estimated as 0.9506.

All the electrochemical studies were performed at least in triplicates under identical conditions unless otherwise stated. The pH of the reaction medium (electrolyte buffer solution) is a crucial parameter because the activity of the immobilized enzyme is dependent on it. The optimum pH for immobilized tyrosinase enzyme is in between 6 to 6.5 (Njagi et al., 2010; Robb and Gutteridge, 1981). Hence, all the experiments have been executed at pH 6.5. Beside this optimization, the number of cyclic voltammetry cycles required to obtain a saturation in the peak current with respect to increasing substrate concentration was found out. It has been after 10th cycle that cathodic peak current (I_{pc}) for *o*-dopaquinone became almost saturated (Figure S2 **in Supplementary Information**). Thus, for all CV measurements, 10th cycle was chosen.

3.2.2. Sensor calibration curve and other parameters

The CV response for Tyrosinase/NiO/ITO electrode has been studied as a function of dopamine concentration (0.1–500 μM) in PBS (50 mM, pH 6.5, 0.9% NaCl) at 100 mV/s scan rate. Fig. 4A shows cathodic (I_{pc}) peak currents for *o*-dopaquinone reduction at −0.16 V and the peak current enhances with increasing concentration of dopamine. This is attributed to the transfer of more electrons during enzymatic reaction with availability of higher concentration of substrate. As shown in the corresponding calibration curve (Fig. 4B), the Tyrosinase/NiO/ITO electrode reveals a linear relationship between magnitudes of peak current for *o*-dopaquinone reduction with dopamine concentration in the range of 2–100 μM and sigmoidal behavior in full concentration range (0.1–500 μM). The following equation was obtained for calibration curve in linear range (Eq. (9))

$$\delta i[\mu A] = 0.1175[\mu A] + 0.0602[\mu A/\mu M] \times \text{concentration } (\mu M)$$
$$\text{with } R^2 = 0.98 \quad (9)$$

The sensitivity of the fabricated electrode has been estimated from slope of the curve and found as 0.0602 μA/μM with linear regression co-efficient (R^2) of 0.98. The flexible electrodes of 1×1 cm^2 area contained an enzyme loading of 11.33 Units of tyrosinase when prepared afresh. The standard deviation and theoretical lower detection limit (LOD, defined as 3 times the sensor noise in plain PBS) are calculated as 0.2087 μA and 1.0375 μM respectively. The calibration curve for whole concentration range (0.1–500 μM) of dopamine detection has been fitted with Hill equation (Fig. 4B inset), with regression coefficient 0.99 and Chi^2/DoF value 2.399×10^{-7}. The sensing parameters of the Tyrosinase/NiO/ITO electrode are compared in Table 1 along with those reported in literature.

3.2.3. Selectivity and response time analysis

In real samples such as human serum, ascorbic acid (AA) and uric acid (UA) co-exist along with dopamine (DA) and show oxidation potentials closer to that of dopamine (Liu et al., 2013; Wang et al., 2009; Zhang et al., 2005). The interference effect of these two substances can be avoided by measuring direct reduction of *o*-dopaquinone during dopamine detection. The immobilized tyrosinase enzyme also helps indirectly in selective detection of dopamine due to enhancement of peak current in presence of dopamine. In the present study, the effects of ascorbic and uric acid on Tyrosinase/NiO/ITO electrode were ascertained (Figure S4 **in Supplementary Information).** The analysis was carried out in PBS (50 mM, pH 6.5, 0.9% NaCl) solution containing equal amount (1:1) of dopamine (100 μM) and either normal physiological concentration or three other different concentrations of interferents, such as ascorbic acid (0.05, 0.5, 0.04 and 0.06 mM), uric acid (0.3, 3, 0.15 and 0.45 mM) and mixture of two interferents (AA 0.05 mM and UA 0.3 mM) and (AA 0.5 mM and UA 3 mM). The amperometric current response for each solution has been compared with control sample (dopamine, 100 μM) using CV studies and the corresponding calibration curve (Fig. 5A). It showed that the fabricated electrode is not considerably affected in presence of

Table 1
Comparison of the fabricated dopamine sensor with other reported tyrosinase/nanoscale material/graphene based dopamine sensors.

Electrode	Method	Linearity (μM)	Sensitivity (μA/μM)	Detection limit (μM)	Ref.
Tyrosinase/Carbon paste	Amperometric	15–250	0.0063	15	(Forzani et al., 1995)
Tyrosinase/Poly(vinyl alcohol) /Ferrocene/Pd/sol-gel	Amperometric	–	0.000125	50	(Pandey et al., 2001)
Tyrosinase/Biocomposite gel (agar-guar gum)/GCE	CV	2–10	–	0.9	(Tembe et al., 2006)
Tyrosinase/MWNT/Nafion/GCE	Amperometric	5–23	0.012	0.52	(Tsai and Chiu, 2007)
Tyrosinase/Glutaraldehyde/Egg-shell membrane	DPV	50–250	–	25	(Tembe et al., 2008)
Graphene/GCE	DPV	4–100	–	2.64	(Kim et al., 2010)
Graphene-Chitosan/GCE	CV	5–200	–	–	(Wang et al., 2009)
CD-MWCNT-poly(luminal)/AuNP/GCE	DPV	1–56	–	0.19	(Jia et al., 2011)
AuNP	UV–visible	0.54–5.4	–	0.36	(Zheng et al., 2011)
CNP/functionalized-silicate particles/ITO	DPV	0.3–18	–	0.36	(Celebanska et al., 2011)
Polycresol red/GCE	LSV	10–100	–	1.5	(Chen et al., 2005)
MWCNT/GCE	DPV	3–300	–	0.8	(Alothman et al., 2010)
Bilayer poly-[β-CD-pyrrole/RGO] /poly-[NEt^{4+}-pyrrole]/tyrosinase	Amperometric	0.027–38.6	0.012	0.027	(Fritea et al., 2015)
Tyrosinase/NiO/ITO	CV	2–100	0.06	1.04	Present work

interfering agents (RSD value ~5–15%). The details of the relative standard deviation with control sample for each solution have given in Table S3 **in Supplementary Information.**

In order to calculate sensor response time, chronoamperometric sensor study was carried out with Tyrosinase/NiO/ITO electrode **(**Figure S5 **in Supplementary Information)** in the time range of 0–180 s with dopamine concentration of 500 μM in PBS (50 mM, pH 6.5, 0.9% NaCl). The 90% of biosensor response was obtained within 45 s, indicating this as the response time of the fabricated sensor.

3.2.4. *Reusability and shelf life studies*

The reproducibility of the biosensor was investigated (Fig. 5B) by repetitive measurements of *o*-dopaquinone reduction peak current in presence of 100 μM dopamine solution in PBS (50 mM, pH 6.5, 0.9% NaCl). Even after 90th measurements, no significant change in sensor response has been observed as evident by low relative standard deviation (RSD = 12.71%). This was perhaps the

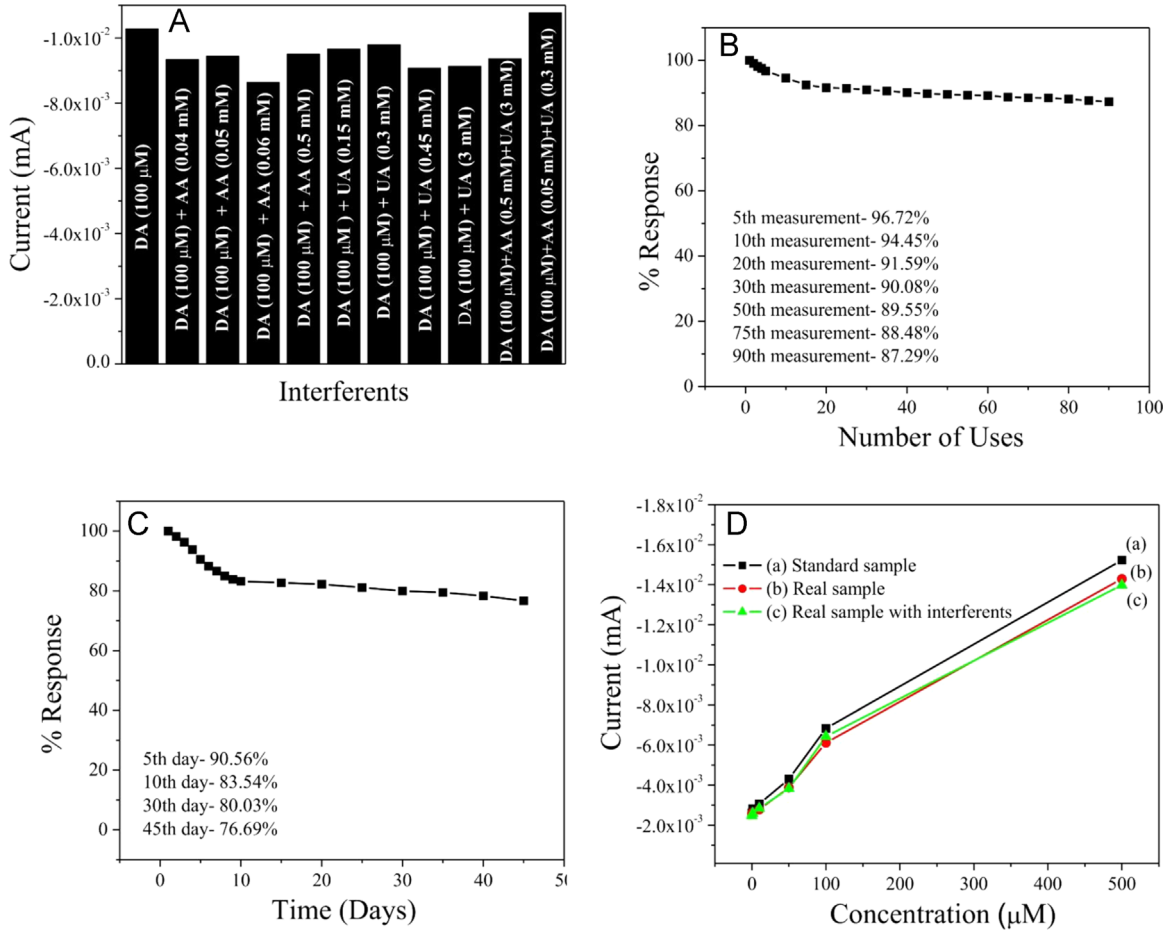

Fig. 5. (A) Selectivity studies on dopamine biosensor in the presence of ascorbic acid (AA) and uric acid (UA); (B) Reusability studies on dopamine biosensor; (C) Shelf-life studies of the fabricated biosensor based on Tyrosinase/NiO/ITO electrode; (D) Detection of dopamine in (a) standard samples, (b) real samples, (c) real samples with the presence of interferents ascorbic acid (0.5 mM) and uric acid (3 mM).

first study in which a dopamine biosensor has been used repetitively with more than 85% of original response until around 100 measurements (extrapolation). The data shows that the enzyme was immobilized onto the nanoparticle surface under optimal conditions, and did not lose its activity while repetitive usage and washing of the matrix. It also suggested that a similar arrangement can be made in a flow through vessel or a microfluidic device for developing a reusable biosensor for neurochemical detection.

The storage stability and shelf life of the fabricated Tyrosinase/NiO/ITO electrode was also monitored (Fig. 5C) by measuring amperometric current response for *o*-dopaquinone at a regular interval of 1 day up to 10 days and then after a gap of 5 days. It has been found that the proposed sensor retains its response by up to 91% after 5 days, 84% after 10 days, 80% after 30 days and falls to 77% after 45 days when stored under refrigerated condition (4 °C). All the reusability experiments were conducted on the same day of electrode preparation and the biosensor showed excellent reusability. However, obtained shelf-life data indicates that a better storage condition has to be evolved for such biosensor, such as storage in moist (Jha et al., 2008) or dry (Kim et al., 2011) conditions to preserve the biosensor for optimal response on the day of use and for point-of-care applications. Nevertheless, the present study shows better shelf-life than previously reported dopamine biosensor (Huang et al., 2014; Zhou et al., 2007).

3.2.5. *Real sample analysis*

In order to demonstrate the applicability and to analyze the matrix effect of biological fluids on the proposed sensor, the detection of dopamine has been conducted by spiking specified concentration of dopamine in fetal bovine serum samples using standard addition method. For that purpose, the fetal bovine serum samples were diluted 15 times with PBS (pH 6.5) and six different concentrations (0.1, 1, 10, 50, 100 and 500 μM) of dopamine were added for measurements. The electrochemical response current were determined for standard samples, serum samples added with particular concentrations of dopamine with or without the presence of excess amount of interferents ascorbic acid (0.5 mM) and uric acid (3 mM). Fig. 5D shows that the magnitude of peak currents obtained for serum samples in or without presence of the interferents are in reasonable agreement with the subsequent standard samples. It can be seen from Table S4 **in Supplementary Information** that adequate recovery values were achieved for both serum samples with or without the interferents. The results also reveal that high content of protein in serum samples have not influenced significantly for dopamine detection with the modified Tyrosinase/NiO/ITO electrode. As the protein content in cerebrospinal fluid (CSF) and other body fluids is much less than fetal bovine serum sample, the proposed sensor can be used precisely for dopamine detection in real samples such as human CSF.

4. Conclusions

In summary, nickel oxide NPs have been synthesized by sol–gel method and successfully functionalized with tyrosinase enzyme molecules to prepare a simple, easy to fabricate, relatively specific, highly reusable and sensitive bio-sensing platform for the detection of neurotransmitter dopamine. The electrochemical response studies of the fabricated electrode showed improved sensitivity (0.0602 μA/μM) for dopamine detection in wide linear detection range (2–100 μM) with fast response time of 45 s due to the presence of stable and highly catalytic NiO NPs that facilitates fast electron transport from bio-recognition element to the underlying ITO substrate. The Tyrosinase/NiO/ITO biosensor exhibits high selectivity for dopamine in presence of ascorbic acid and uric acid (RSD value ~5–15%), long-term stability (45 days) with excellent reusability. Since the whole sensing strip was built on a flexible substrate and could be successfully demonstrated for its ability of dopamine sensing, therefore, the fabricated Tyrosinase/NiO/ITO electrode has the potential to be developed into a handheld platform for dopamine or similar neurochemical detection and can be used in point-of-care applications.

Acknowledgments

The work was supported by a research grant from Department of Biotechnology, Government of India (Grant No. BT/PR7190/PID/6/719/2012). The author Appan Roychoudhury is a recipient of Junior Research Fellowship from Indian Institute of Technology Delhi.

Appendix A. Supplementary material

Supplementary data associated with this article can be found in the online version at http://dx.doi.org/10.1016/j.bios.2015.11.061.

References

Ali, M.A., Solanki, P.R., Patel, M.K., Dhayani, H., Agrawal, V.V., John, R., Malhotra, B.D., 2013. Nanoscale 5, 2883–2891.
Alothman, Z.A., Bukhari, N., Wabaidur, S.M., Haider, S., 2010. Sens. Actuators B Chem. 146, 314–320.
Arslan, A., Kiralp, S., Toppare, L., Yagci, Y., 2005. Int. J. Biol. Macromol. 35, 163–167.
Barreto, W.J., Barreto, S.R.G., Ando, R.A., Santos, P.S., DiMauro, E., Jorge, T., 2008. Spectrochim. Acta-Part A Mol. Biomol. Spectrosc. 71, 1419–1424.
Beitollahi, H., Karimi-Maleh, H., Khabazzadeh, H., 2008. Anal. Chem. 80, 9848–9851.
Cao, X., Luo, L., Ding, Y., Zou, X., Bian, R., 2008. Sens. Actuators B Chem. 129, 941–946.
Carrera, V., Sabater, E., Vilanova, E., Sogorb, M.A., 2007. J. Chromatogr. B Anal. Technol. Biomed. Life Sci. 847, 88–94.
Caruso, C.S., da Cruz Vieira, I., Fatibello-Filho, O., 1999. Anal. Lett. 32, 39–50.
Caruso, F., 2001. Adv. Mater. 13, 11–22.
Celebanska, A., Tomaszewska, D., Lesniewski, A., Opallo, M., 2011. Biosens. Bioelectron. 26, 4417–4422.
Chen, J.-L., Yan, X.-P., Meng, K., Wang, S.-F., 2011. Anal. Chem. 83, 8787–8793.
Chen, S.-M., Peng, K.-T., 2003. J. Electroanal. Chem. 547, 179–189.
Chen, W., Lin, X., Huang, L., Luo, H., 2005. Microchim. Acta 151, 101–107.
Daigle, F., Leech, D., 1997. Anal. Chem. 69, 4108–4112.
Deftereos, N.T., Calokerinos, A.C., Efstathiou, C.E., 1993. Analyst 118, 627–632.
Doong, R., Shih, H., 2010. Biosens. Bioelectron. 25, 1439–1446.
El-Beqqali, A., Kussak, A., Abdel-Rehim, M., 2007. J. Sep. Sci. 30, 421–424.
Forzani, E.S., Rivas, G.A., Solis, V.M., 1995. J. Electroanal. Chem. 382, 33–40.
Fritea, L., Goff, A.L., Putaux, J.-L., Tertis, M., Cristea, C., Săndulescu, R., Cosnier, S., 2015. Electrochim. Acta 178, 108–112.
Furbee Jr, J.W., Thomas, C.R., Kelly, R.S., Malachowski, M.R., 1993. Anal. Chem. 65, 1654–1657.
Heien, M.L., Khan, A.S., Ariansen, J.L., Cheer, J.F., Phillips, P.E., Wassum, K.M., Wightman, R.M., 2005. Proc. Natl. Acad. Sci. USA 102, 10023–10028.
Huang, Q., Zhang, H., Hu, S., Li, F., Weng, W., Chen, J., Wang, Q., He, Y., Zhang, W., Bao, X., 2014. Biosens. Bioelectron. 52, 277–280.
Huffman, M.L., Venton, B.J., 2009. Analyst 134, 18–24.
Jha, S.K., Topkar, A., D'Souza, S.F., 2008. J. Biochem. Biophys. Methods 70, 1145–1150.
Jia, D., Dai, J., Yuan, H., Lei, L., Xiao, D., 2011. Talanta 85, 2344–2351.
Justin, P., Meher, S.K., Rao, G.R., 2010. J. Phys. Chem. C. 114, 5203–5210.
Kang, J., Yin, X.-B., Yang, X., Wang, E., 2005. Electrophoresis 26, 1732–1736.
Kavitha, T., Yuvaraj, H., 2011. J. Mater. Chem. 21, 15686–15691.
Khattar, R., Mathur, P., 2013. Inorg. Chem. Commun. 31, 37–43.
Kim, J.-M., Jha, S.K., Lee, D.-H., Chand, R., Jeun, J.-H., Sin, I.-S., Kim, Y.-S., 2011. Micro Nano Lett. 6, 745–748.
Kim, Y.-R., Bong, S., Kang, Y.-J., Yang, Y., Mahajan, R.K., Kim, J.S., Kim, H., 2010. Biosens. Bioelectron. 25, 2366–2369.
Koile, R.C., Johnson, D.C., 1979. Anal. Chem. 51, 741–744.
Laviron, E., 1979. J. Electroanal. Chem. Interfacial Electrochem. 101, 19–28.
Li, C., Liu, Y., Li, L., Du, Z., Xu, S., Zhang, M., Yin, X., Wang, T., 2008. Talanta 77, 455–459.
Li, H., Li, C., Yan, Z., Yang, J., Chen, H., 2010. J. Neurosci. Methods 189, 162–168.
Liu, A., Honma, I., Zhou, H., 2005. Electrochem. Commun. 7, 233–236.
Liu, M., Chen, Q., Lai, C., Zhang, Y., Deng, J., Li, H., Yao, S., 2013. Biosens. Bioelectron.

48, 75–81.
Matos, R.C., Angnes, L., Araújo, M.C., Saldanha, T.C., 2000. Analyst 125, 2011–2015.
Mecker, L.C., Martin, R.S., 2008. Anal. Chem. 80, 9257–9264.
Mo, J.-W., Ogorevc, B., 2001. Anal. Chem. 73, 1196–1202.
Mohan, S., Srivastava, P., Maheshwari, S.N., Sundar, S., Prakash, R., 2011. Analyst 136, 2845–2851.
Muzzi, C., Bertocci, E., Terzuoli, L., Porcelli, B., Ciari, I., Pagani, R., Guerranti, R., 2008. Biomed. Pharmacother. 62, 253–258.
Myers, R.D., Adell, A., Lankford, M.F., 1998. Neurosci. Biobehav. Rev. 22, 371–387.
Nikolelis, D.P., Drivelos, D.A., Simantiraki, M.G., Koinis, S., 2004. Anal. Chem. 76, 2174–2180.
Nistor, C., Emnéus, J., Gorton, L., Ciucu, A., 1999. Anal. Chim. Acta 387, 309–326.
Njagi, J., Chernov, M.M., Leiter, J.C., Andreescu, S., 2010. Anal. Chem. 82, 989–996.
Pandey, P.C., Upadhyay, S., Tiwari, I., Singh, G., Tripathi, V.S., 2001. Sens. Actuators B Chem. 75, 48–55.
Rajesh, Takashima, Kaneto, K., W., 2004. React. Funct. Polym. 59, 163–169.
Robb, D.A., Gutteridge, S., 1981. Phytochemistry 20, 1481–1485.
Robinson, D.L., Venton, B.J., Heien, M.L., Wightman, R.M., 2003. Clin. Chem. 49, 1763–1773.
Salimi, A., Sharifi, E., Noorbakhsh, A., Soltanian, S., 2007. Biophys. Chem. 125, 540–548.
Singh, J., Roychoudhury, A., Srivastava, M., Chaudhary, V., Prasanna, R., Lee, D.W., Lee, S.H., Malhotra, B.D., 2013. J. Phys. Chem. C. 117, 8491–8502.
Singh, M.K., Agarwal, A., Gopal, R., Swarnkar, R.K., Kotnala, R.K., 2011. J. Mater. Chem. 21, 11074–11079.
Smith, N., 1936. J. Am. Chem. Soc. 58, 173–179.
Solanki, P.R., Kaushik, A., Agrawal, V.V., Malhotra, B.D., 2011. NPG Asia Mater. 3, 17–24.
Tembe, S., Karve, M., Inamdar, S., Haram, S., Melo, J., D'Souza, S.F., 2006. Anal. Biochem. 349, 72–77.
Tembe, S., Kubal, B.S., Karve, M., D'Souza, S.F., 2008. Anal. Chim. Acta 612, 212–217.
Thabano, J.R., Breadmore, M.C., Hutchinson, J.P., Johns, C., Haddad, P.R., 2009. J. Chromatogr. A 1216, 4933–4940.
Thanh, N.T.K., Green, L.A.W., 2010. Nano Today 5, 213–230.
Tsai, Y.-C., Chiu, C.-C., 2007. Sens. Actuators, B Chem. 125, 10–16.
Umasankar, Y., Chen, S.-M., 2008. Sens. Actuators, B Chem. 130, 739–749.
Wang, Y., Li, Y., Tang, L., Lu, J., Li, J., 2009. Electrochem. Commun. 11, 889–892.
Wightman, R.M., May, L.J., Michael, A.C., 1988. Anal. Chem. 60, 769A–779A.
Zhang, M., Gong, K., Zhang, H., Mao, L., 2005. Biosens. Bioelectron. 20, 1270–1276.
Zhang, Y., Ren, W., Zhang, S., 2013. Int. J. Electrochem. Sci. 8, 6839–6850.
Zheng, Y., Wang, Y., Yang, X., 2011. Sens. Actuators, B Chem. 156, 95–99.
Zhou, Y.L., Tian, R.H., Zhi, J.F., 2007. Biosens. Bioelectron. 22, 822–828.

Please cite this article as: Roychoudhury, A., et al., Biosensors and Bioelectronics (2015), http://dx.doi.org/10.1016/j.bios.2015.11.061